GLRT Particle Filter for Non-Line of Sight Single Moving Target Tracking via Phased Array Radar

Ba-Huy Pham, Olivier Rabaste, Jonathan Bosse, Israel Hinostroza, Thierry Chonavel

GLRT Particle Filter for Non-Line of Sight Single Moving Target Tracking via Phased Array Radar

Ba-Huy Pham[1,2], Olivier Rabaste[1], Jonathan Bosse[1], Israel Hinostroza[2], Thierry Chonavel[3]
[1] DEMR, ONERA, Université Paris-Saclay, F-91123 Palaiseau, France
[2] SONDRA, CentraleSupelec, Université Paris-Saclay, F-91192 Gif-sur-Yvette, France
[3] IMT Atlantique, Lab-STICC, UMR CNRS 6285, F-29238 Brest, France

***Abstract*—In around the corner radar, particle filter tracking can help to improve the estimation accuracy of a Non-Line of Sight target position. However, in case of using one single receiving antenna, the measurement model only contains multipath delay information. Due to the lack of information in the model, particles corresponding to ambiguous positions can be assigned high weight values. This can leads the particle cloud to diverge from the actual target trajectory and requires several time steps to converge on it again. In this work, our proposed solution consists in exploiting additional Direction-of-Arrival information provided by an array of receiving antennas in the particle filter framework. By simulation and experimentation, we will show that the proposed solution allows to solve the aforementioned problem, and thus achieves better localization results compared to single antenna-based tracking as well as non-tracking localization algorithm.**

***Index Terms*—NLOS target tracking, particle filter, around-the-corner radar, multipath, ambiguities, ray tracing simulation.**

I. Introduction

Detection and localization of targets in urban settings is a relatively new area of study in radar applications. The presence of buildings creates shadow areas where targets are not visible in light of sight of the radar (NLOS). However, targets in these NLOS areas can still be detected by exploiting multipaths produced by reflections on surrounding surfaces. These multipaths often pose a challenge in classical radar applications. But in urban radar applications, radar information carried by multipaths represent an opportunity to locate and track NLOS targets. This technique is called "around-the-corner radar" [1]. First papers on this topic have demonstrated, via experiments its feasibility [1]- [3]. Then, several works [4]-[6], have proposed different methods for target localization based on parameters association.

Especially, the authors of [7] proposed a joint detection and localization algorithm of a target using the Matched Subspace Filter (MSF) [8], derived from the Maximum Likelihood (ML) criterion. This method enables to detect and locate directly in the target space [9], by exploiting the multipath delay information provided by a simple ray tracing model and a rough knowledge of the scene geometry. To assess the localization performance, the authors of [7] applied the algorithm on experimental data using a handheld radar system having a single receiving antenna. Although the estimation of the target position is accurate most of the time, estimation error is still significant. Indeed, the use of a single receiving antenna only provides multipath delay-only information. Due to the geometry configuration, ghost positions may share several common delays with the true target position in their model. As a result, they are assigned high likelihood values at the MSF output, thus are likely to create estimation bias, especially when paths signal-to-noise ratio (SNR) is low.

To deal with this problem, called localization ambiguity in [7], the authors of [10] adopted the tracking approach, for instance using the particle filter. The simple idea behind is to exploit the dynamics of the target over several radar measurements to remove the ghost positions which are not relevant and are not belonging to the target track. The use of a particle filter was justified by the high non-linearity of the measurement model [11], since multipath radar parameters are linked to the target position states by unknown and complex geometrical relations that are specific to each scenario. Moreover, the Generalized Likelihood Ratio Test (GLRT) particle filter algorithm, first introduced in [12] in the Track-Before-Detect framework, has been chosen for implementation in [10]. It is designed to circumvent the disadvantages of sampling multipath amplitude by replacing it with its ML estimator. Interestingly, particle weight update is straightforwardly proportional the MSF cost function. By simulations, the GLRT particle filter has been shown to achieve higher estimation accuracy compared to a localization algorithm without tracking using the MSF approach in [7].

Despite its straightforward implementation, the GLRT particle filter performance is highly sensitive to the state initialization. Indeed, particles located at MSF ghost positions will be equivalently granted high weight values. This becomes problematic when these heavily weighted particles attract the particle cloud to converge too far from the true target trajectory. Worst still, the well known resampling mechanism of the particle filter can exacerbate the situation: it tends to confine the misled cloud around ghost positions. For this reason, the filter needs several time steps before correcting this estimation bias, then likely leading to low convergence rate.

In this work, we present a solution for the above described problem of the GLRT particle filter by using an array of receiving antennas which provides additional Direction-of-

Arrival (DoA) information. Indeed, the idea of exploiting DoA information has been introduced in [13] for the non-tracking MSF localization approach, which has shown a significant reduction of ghost positions level at the MSF output. It is worthwhile to integrate this additional information into the particle filter framework with the aim of reducing the weight of ghost position particles, then improving the estimation results. Both simulated and experimental results obtained with the proposed multiple receiving antenna particle filter show that it can achieve higher convergence rate and robustness compared to single antenna-based tracking [10], thus better localization results.

The article is organized as follows. In Section 2, state and measurement models will be presented. In Section 3, we will present proposed particle filter for NLOS tracking. Section 4 provides the experimentation setup and localization results on both simulated and real data. The last section is dedicated to the conclusion and perspectives.

II. Modelling

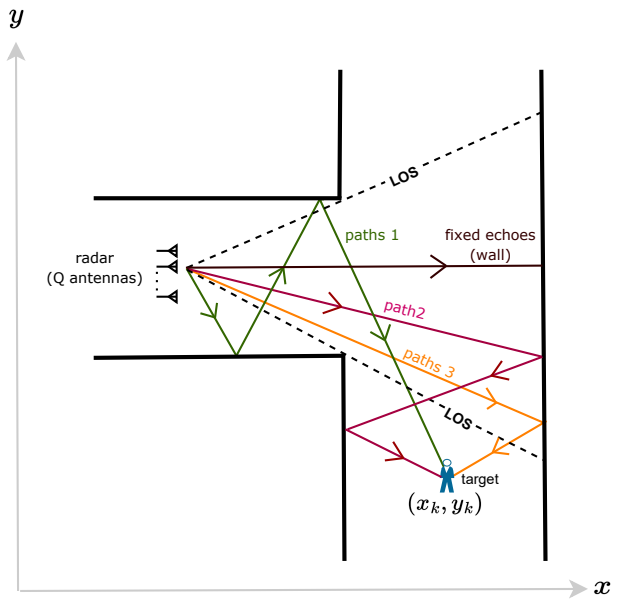

Fig. 1: The urban scenario

Let us introduce the framework by first considering a simple scenario: an urban intersection as depicted in Fig. 1. Only a rough knowledge of the 2D scene geometry is required, namely the coordinates of the building walls. The radar system is placed into the scene, which is composed of a single transmitting (Tx) antenna and a linear array of Q receiving (Rx) antennas. At each radar measurement, a signal $s(t)$, with bandwidth B and carrier frequency f_c is transmitted by the Tx antenna. In this study, we only consider high frequency band radar system, for instance $f_c \geq 10$ GHz, so that electromagnetism (EM) multipath propagation in the given scene can be well approximated by the ray tracing model. Here, only specular reflection paths are considered, as illustrated in Fig. 1. Diffraction paths are supposed to be too weak regarding the considered radar operating frequency range.

Despite the specific configuration described above, the model as well as the solutions derived in the sequel can be easily extended to any other scene geometry or EM propagation models supported by more realistic simulation tools.

A. State model

Here, we tackle the problem of tracking a single moving target. Specifically, at discrete time $k \in \mathbb{N}$, the target dynamic state is characterized by the state vector $\mathbf{x}_k = [x_k, y_k, \dot{x}_k, \dot{y}_k]^T$ which includes both the target current position in Cartesian coordinates (x_k, y_k) and its velocity components $(\dot{x}_k, \dot{y}_k)$. The dynamic model of the target is then represented by the following linear state equation:

$$\mathbf{x}_k = \mathbf{F}_k \mathbf{x}_{k-1} + \mathbf{v}_k, \tag{1}$$

where

$$\mathbf{F}_k = \begin{bmatrix} 1 & 0 & T_m & 0 \\ 0 & 1 & 0 & T_m \\ 0 & 0 & 1 & 0 \\ 0 & 0 & 0 & 1 \end{bmatrix} \tag{2}$$

is the transition matrix that depends on the discretization time T_m, that represents the duration between 2 consecutive radar measurements. Hence, for the rest of the paper, k will interchangeably designate the discret time and the measurement number. The variable $\mathbf{v}_k$ represents the process noise vector which is assumed to be white Gaussian with known covariance matrix $\mathbf{Q}_s = \sigma_s^2 \mathbf{I}$.

B. Measurement model

At each radar measurement k, we propose a scheme where the multipath received signal is collected by the Q antennas of the Rx array. Let us assume that paths corresponding to fixed echoes returned from different reflecting walls are first removed from the received signal by a classic zero-Doppler cancellation filter, leaving only the contribution of the multipath signals from the target. Then, for the sake of simplicity, we will also neglect the Doppler shift term in the measurement model, although we keep in mind that this information has been exploited for fixed echoes cancellation.

Under these assumptions, the signal received from the target of interest by the q-th Rx antenna at time k is given by

$$y_{q,k}(t) = \sum_{m=1}^{M(x_k,y_k)} \alpha_{m,k}\, s\left(t - \tau_m(x_k, y_k)\right) e^{j\mathbf{k}_{\theta_m(x_k,y_k)}^T \mathbf{p}_q} + w_{q,k}(t), \tag{3}$$

where $M(x_k, y_k)$ denotes the number of multipaths provided by the ray tracing model for the target current position coordinates (x_k, y_k). $\alpha_{m,k}$ is the complex amplitude of path m, assumed to be unknown. $\tau_m(x_k, y_k), \theta_m(x_k, y_k)$ are the round-trip delay and DoA of path m, respectively, and are provided by the ray tracing model. $\mathbf{k}_\theta$ is the wave vector

in the path receiving direction θ. $\mathbf{p}_q$ denotes Cartesian coordinate position vector for q-th antenna. $w_{q,k}(t)$ represents the observation noise on this antenna, assumed to be complex circular complex white Gaussian with known variance σ_n^2. The matched filter to the reference signal $s(t)$ is first applied on $y_{k,q}$ and yields

$$z_{q,k}(t) = \sum_{m=1}^{M(x_k,y_k)} \alpha_{m,k} r(t - \tau_m(x_k, y_k)) e^{j\mathbf{k}_{\theta_m(x_k,y_k)}^T \mathbf{p}_q} + n_{q,k}(t), \tag{4}$$

where $z_{q,k}(t)$, $n_{q,k}(t)$ are obtained by correlating $y_{q,k}(t)$, $w_{q,k}(t)$ with $s(t)$ and $r(t)$ is the auto-correlation of $s(t)$. Then, sampling each $z_{q,k}(t)$ at time period $t_s = 1/B$, we obtain the N-dimensional observation vector:

$$\mathbf{z}_{q,k} = [z_{q,k}(t_s), z_{q,k}(2t_s), \ldots, z_{q,k}(Nt_s)]^T. \tag{5}$$

Stacking the observation vectors $\mathbf{z}_{q,k}$ of all Q Rx antennas, we obtain the measurement equation at time k:

$$\mathbf{z}_k = \mathbf{R}(x_k, y_k)\boldsymbol{\alpha}_k + \mathbf{n}_k, \tag{6}$$

where

$$\mathbf{z}_k = \left[\mathbf{z}_{1,k}^T, \mathbf{z}_{2,k}^T, \ldots, \mathbf{z}_{Q,k}^T\right]^T, \tag{7}$$

$$\mathbf{n}_k = \left[\mathbf{n}_{1,k}^T, \mathbf{n}_{2,k}^T, \ldots, \mathbf{n}_{Q,k}^T\right]^T, \tag{8}$$

$$\boldsymbol{\alpha}_k = \left[\alpha_{1,k}, \alpha_{2,k}, \ldots, \alpha_{M(x_k,y_k),k}\right]^T,$$

$$\mathbf{R}(x_k, y_k) = \left[\mathbf{r}_1(x_k, y_k), \ldots, \mathbf{r}_{M(x_k,y_k)}(x_k, y_k)\right]. \tag{9}$$

Each column $\mathbf{r}_m(x_k, y_k)$ of $\mathbf{R}(x_k, y_k)$ corresponds to a characteristic multipath vector for the target position (x_k, y_k):

$$\mathbf{r}_m(x_k, y_k) = \mathbf{r}(\tau_m(x_k, y_k)) \otimes \mathbf{a}(\theta_m(x_k, y_k)), \tag{10}$$

where

$$\mathbf{r}(\tau) = [r(t_s - \tau), r(2t_s - \tau) \ldots, r(Nt_s - \tau)], \tag{11}$$

and $\mathbf{a}(\theta_m(x_k, y_k)) = \left[e^{j\mathbf{k}_{\theta_m(x_k,y_k)}^T \mathbf{p}_1}, \ldots, e^{j\mathbf{k}_{\theta_m(x_k,y_k)}^T \mathbf{p}_Q}\right]^T$ denotes the steering vector for the direction $\theta_m(x_k, y_k)$. The operator $\otimes$ represents the Kronecker product.

The measurement model in (6) can be seen as an extension of the model presented [10] in order to cover multiple antennas scheme. In case of a single Rx antenna, i.e., $Q = 1$, the measurement model boils down to that presented in [10]. It can also be highlighted that the measurement equation here is highly non-linear. Worse still, the observation vector $\mathbf{z}_k$ is not related to the state variables (x_k, y_k) by any explicit function, but through the parameters $\tau_m(x_k, y_k)$ and $\theta_m(x_k, y_k)$ of each characteristic multipath $\mathbf{r}_m(x_k, y_k)$ in the matrix $\mathbf{R}(x_k, y_k)$. These parameters, in turn, are linked to (x_k, y_k) by a complex geometrical relation specific to each scene, that can only be retrieved for instance via ray tracing simulation. Note that the number of characteristic multipath vectors $M(x_k, y_k)$, that is the number of columns of $\mathbf{R}(x_k, y_k)$ and $\boldsymbol{\alpha}_k$ also depend on the target position (x_k, y_k).

III. GLRT PARTICLE FILTER TRACKING ALGORITHM

Since the particle filter is a suitable approach for addressing non-linearity, it is adopted here for the target tracking problem. In order to implement the particle filter, the measurement likelihood should be computed conditionally to the target state. However, amplitude vector $\boldsymbol{\alpha}_k$ depends on the target position (x_k, y_k). However, $\boldsymbol{\alpha}_k$ information is unknown and can not be retrieved from the ray tracing model. Indeed, multipath amplitude modelling is generally involved due to the lack of knowledge about propagation environment factor, such as the propagation losses, the reflection coefficient on each reflective surface, target aspect angle, etc. Classical particle filter strategy deals with unknown amplitude vector by including it to the particle states [14]. In our case, this yields the augmented state vector $\mathbf{X}_k = \left[(\mathbf{x}_k)^T, (\boldsymbol{\alpha}_k)^T\right]^T$.

Now we seek to approximate the posterior density function $p(\mathbf{X}_k|\mathbf{z}_{1:k})$ by a cloud of N_p weighted particles $\left\{\mathbf{X}_k^i, w_k^i\right\}_{i=1}^{N_p}$. The state $\mathbf{X}_k^i$ of each particle i consists of

$$\mathbf{X}_k^i = \left[\left(\mathbf{x}_k^i\right)^T, \left(\boldsymbol{\alpha}_k^i\right)^T\right]^T = \left[x_k^i, y_k^i, \dot{x}_k^i, \dot{y}_k^i, \left(\boldsymbol{\alpha}_k^i\right)^T\right]^T. \tag{12}$$

Particles are propagated from time $k-1$ to time k via 2 steps procedure: first new particle states $\mathbf{X}_k^i$ are drawn from their previous states $\mathbf{X}_{k-1}^i$ according to a proposal importance density $q\left(\mathbf{X}_k^i|\mathbf{X}_{k-1}^i, \mathbf{z}_{1:k}\right)$. Second, unnormalized particle weights are updated via the following equation [11]:

$$\tilde{w}_k^i \propto w_{k-1}^i \frac{p\left(\mathbf{z}_k|\mathbf{X}_k^i\right) p\left(\mathbf{X}_k^i|\mathbf{X}_{k-1}^i\right)}{q\left(\mathbf{X}_k^i|\mathbf{X}_{k-1}^i, \mathbf{z}_{1:k}\right)}. \tag{13}$$

Though a classical particle filter would sample the target amplitude according to the prior model, this strategy presents two drawbacks: first it assumes a coherent behavior of the amplitude along time enabling to describe it via a Markov chain model, that is unrealistic in our context. Second, amplitude parameter implies increasing considerably the state space dimension, thus the number of required particles [12]. In order to circumvent the amplitude sampling, we seek to replace amplitude parameter with its Maximum Likelihood (ML) estimator. To do this, first we propose to factorize the importance density as proposed in [12]:

$$q\left(\mathbf{X}_k^i|\mathbf{X}_{k-1}^i, \mathbf{z}_{1:k}\right) = q\left(\boldsymbol{\alpha}_k^i|\mathbf{x}_k^i, \mathbf{z}_k\right) p\left(\mathbf{x}_k^i|\mathbf{X}_{k-1}^i\right). \tag{14}$$

This means that the position and velocity of the target are sampled according to the state equation, while the multipath amplitude vector is sampled conditionally to the target position and velocity at time k and to the observation at time k. Here, we choose the following importance density for amplitude variable as proposed in [10]:

$$q\left(\boldsymbol{\alpha}_k^i|\mathbf{x}_k^i, \mathbf{z}_{1:k}\right) \sim \mathcal{N}\left(\hat{\boldsymbol{\alpha}}_k^i, \sigma_{\boldsymbol{\alpha}}^2 \mathbf{I}_{M(x_k^i, y_k^i)}\right), \tag{15}$$

where $\hat{\boldsymbol{\alpha}}_k^i$ denotes the ML estimator of the particle amplitude $\boldsymbol{\alpha}_k^i$ given by:

$$\hat{\boldsymbol{\alpha}}_k^i = \left[\mathbf{R}(x_k^i, y_k^i)^H \mathbf{R}(x_k^i, y_k^i)\right]^{-1} \mathbf{R}(x_k^i, y_k^i)^H \mathbf{z}_k, \tag{16}$$

and $\sigma^2_{\boldsymbol{\alpha}}$ is an adjustable variance of the amplitude variable and $M(x^i_k, y^i_k)$ is the number of multipaths corresponding to the position of the particle $\mathbf{X}^i_k$. Considering the specific case in which $\sigma^2_{\boldsymbol{\alpha}} \to 0$, the amplitude importance density becomes a point mass distribution, i.e., $q\left(\boldsymbol{\alpha}^i_k | \mathbf{x}^i_k, \mathbf{z}_{1:k}\right) = \delta_{\hat{\boldsymbol{\alpha}}^i_k}(\boldsymbol{\alpha}^i_k)$. This means sampling $\boldsymbol{\alpha}^i_k$ from $q\left(\boldsymbol{\alpha}^i_k | \mathbf{x}^i_k, \mathbf{z}_{1:k}\right)$ directly yields its ML estimator. Hence, the weights update (13) becomes

$$\tilde{w}^i_k \propto w^i_{k-1} \exp\left(-\frac{\|\mathbf{z}_k - \mathbf{R}\left(x^i_k, y^i_k\right)\hat{\boldsymbol{\alpha}}^i_k\|^2}{\sigma^2_n}\right), \qquad (17)$$

that yields the GLRT particle filter proposed in [12]. Here the quantity $\exp\left(-\frac{\|\mathbf{z}_k - \mathbf{R}\left(x^i_k, y^i_k\right)\hat{\boldsymbol{\alpha}}^i_k\|^2}{\sigma^2_n}\right)$ is proportional to the likelihood of the observation given the multipath model at position (x^i_k, y^i_k), known as Matched Subspace Filter (MSF) [8]. The latter yields the Maximum Likelihood (ML) criterion that is used in [7] to locate the target, based on a single observation. Particles weights are then normalized so that $\sum_{i=1}^{N_p} w^i_k = 1$. After normalization, a resampling step might be necessary to avoid particle degeneracy [11]. The usual criteria for resampling is provided by an estimate of the number of effective particles $\hat{N}_{\text{eff}} = 1/\sum_{i=1}^{N_p}(w^i_k)^2$ that is compared to a threshold N_{thres}. The discrete approximation of the posterior density up to time k by the particle cloud is given by

$$p(\mathbf{X}_k | \mathbf{z}_{1:k}) \approx \sum_{i=1}^{N_p} w^i_k \delta_{\mathbf{X}^i_k}(\mathbf{X}_k). \qquad (18)$$

Then it is possible to retrieve an estimate of the target position at time k, for instance using a classical Minimum Mean Square Error (MMSE) estimator

$$\hat{x}_k = \frac{1}{N_p}\sum_{i=1}^{N_p} w^i_k x^i_k \text{ and } \hat{y}_k = \frac{1}{N_p}\sum_{i=1}^{N_p} w^i_k y^i_k. \qquad (19)$$

The particle filter for NLOS target tracking is summarized in Algorithm 1.

Algorithm 1 Particle filter for NLOS target tracking

Require: Particle cloud $\left\{\mathbf{X}^i_{k-1}, w^i_{k-1}\right\}_{i=1}^{N_p}$ at step $k-1$
for i = 1 to N_p **do**
  Draw $\mathbf{x}^i_k$ according to $p\left(\mathbf{x}^i_k | \mathbf{x}^i_{k-1}\right)$
  Draw $\boldsymbol{\alpha}^i_k$ by computing its ML estimator $\hat{\boldsymbol{\alpha}}^i_k$ according to (16)
  Update weight $\tilde{w}^i_k \propto w^i_{k-1} \exp\left(-\frac{\|\mathbf{z}_k - \mathbf{R}\left(x^i_k, y^i_k\right)\hat{\boldsymbol{\alpha}}^i_k\|^2}{\sigma^2_n}\right)$
end for
Normalize weights:
for i = 1 to N_p **do**
  $w^i_k \leftarrow \frac{\tilde{w}^i_k}{\sum_{i=1}^{N_p}\tilde{w}^i_k}$
end for
Compute $\hat{N}_{\text{eff}} = 1/\sum_{i=1}^{N_p}(w^i_k)^2$
if $\hat{N}_{\text{eff}} < N_{\text{thres}}$ **then**
  Resample N_p particles
  Reset weights $w^i_k \leftarrow \frac{1}{N_p}$
end if
return $\left\{\mathbf{X}^i_k, w^i_k\right\}_{i=1}^{N_p}$

IV. Experimental results

In this section, we propose an experiment using a radar system with a linear antenna array, performed in a realistic urban scenario. The collected data are used to assess the localization performance of the particle filter (PF) in case of exploiting multipath information from multiple Rx antennas (delay and DoA) as presented in the previous sections in comparison with the case of using a single Rx antenna (delay only) presented in [10]. We will also compare the localization results of the particle filter with the non-tracking localization algorithm based on the Matched Subspace Filer (MSF), presented in [7] and [13].

A. Experiment description

1) Measuring equipment: the radar system used for the experiment is the EVAL-TINYRAD FMCW [16]. It has a linear array of $Q = 4$ receiving antennas where the element spacing is one-half of the wavelength, which results in an angular resolution $\Delta_\theta \approx 28°$. The signal $s(t)$, composed by a train of pulses, is transmitted towards the scene by one single Tx antenna. Each elementary pulse is a chirp signal with carrier frequency $f_c = 24.05$ GHz and bandwidth $B = 235$ MHz, thus yielding a radar range resolution $\Delta_r = c/B = 1.3$ m. The pulse repetition interval and the number of pulses are set to $PRI = 200$ and $N_{\text{pulses}} = 400$, which results in Doppler velocity resolution $\Delta_v = 0.07$ m/s.

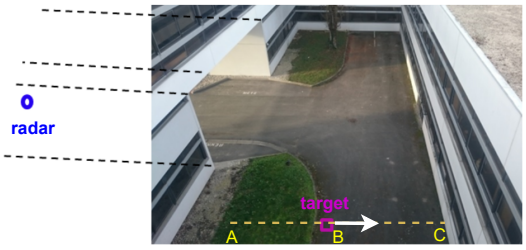

Fig. 2: Urban scene photo

2) Experiment scenario: the considered urban scene is a T-junction, photo of which is displayed in Fig. 2. The walls 2D-coordinates are then transcribed in the ray tracing simulator as shown in Fig. 3. The radar system is placed at the coordinates $(4.26; 5.94)$. The target is a pedestrian, first located at $A(15.88, -5.05)$, starts moving up to $C(25.41, -5.05)$ in which he appears in LOS at $B(20.58, -5.05)$. 61 measurements have been recorded at a $T_m = 80$ ms interval, that covers the total duration of the target movement.

3) Preprocessing: for each measurement k, in order to obtain the observation vector from the received radar raw signal of each Rx receiving antenna q, first, fixed echoes are cancelled by filtering out all zero-Doppler components from the signal spectrum. Then, range and Doppler matched filters are applied, yielding the range-Doppler 2D-FFT matrix. The

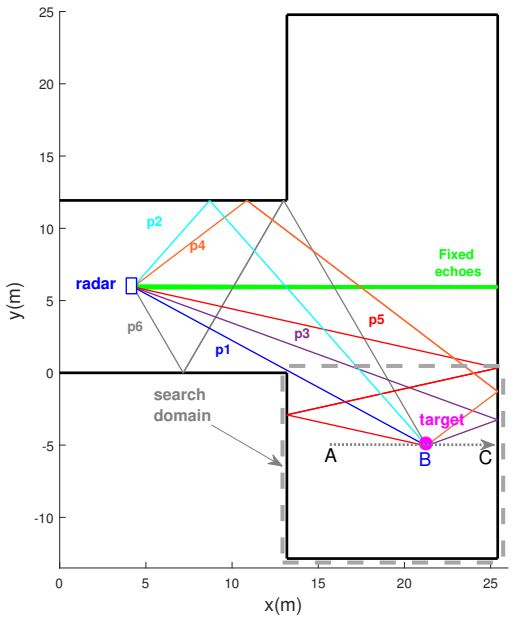

Fig. 3: The ray tracing simulation performed for the experiment scenario.

range-dependent only observation vector $\mathbf{z}_q$ is extracted from the range-Doppler matrix by selecting, for each range bin, the corresponding Doppler bin with highest peak. This can be done under the assumption that each path only occupies a single range-Doppler bin with dominant magnitude. Fig. 4a presents the observation vectors for one Rx antenna over 61 measurements. Here, it is possible to identify different rays in Fig. 3, where p_{ab} refers to the multipath which goes from the radar to the target through path a and back through path b.

In order to compare with the real data, we also simulated the same scenario as described above, thus obtaining the simulated observation vectors as displayed in Fig. 4c. In the simulation, it is assumed that the direct path SNR is roughly 30 dB, in view of its maximum SNR value from the real data. Based on the direct path energy, multipath energy losses are simulated with propagation loss inversely proportional to the path propagation distance and reflection loss of -5 dB per reflection.

One can note that in case of 4 Rx antennas, the resulting paths SNR is 6 dB larger than in the one Rx antenna case. However, to have a fair comparison, it is preferable that the paths SNR be the same in both cases. Hence, we subsequently consider that the observation vector in the single antenna case, on which will be applied localization algorithms, is obtained by integrating the observation vectors from 4 Rx antennas coherently.

B. Particle filter setting

At first glance, the linear evolution of the target range profile shown in Fig. 4a is relevant to the linear uniform state model in (1). The state noise is empirically set to $\sigma_s^2 = 0.1$. Position states (x, y) is initialized in the search domain defined in Fig. 3 whereas particle velocities (v_x, v_y) are evenly drawn from the interval $[-2, 2]$ m.s^{-1}, based on the assumption of the pedestrian radial velocity. Hence, at $k = 0$, particles $\mathbf{x}_k^0$ are initialized uniformly over all the space (x, y, v_x, v_y). All particle weights are initialized to $w_0^i = 1/N_p$.

In addition, we note that computing the particles weights at each time step k requires obtaining in real time the matrix $\mathbf{R}\left(x_k^i, y_k^i\right)$ corresponding to each particle position $\left(x_k^i, y_k^i\right)$ via ray tracing simulations, which would imply an extremely high computational cost. To circumvent this drawback, the search domain is first finely discretized into $J = 6155$ cells of size 0.16×0.16 m, which is equal to one eighth of the range resolution. Then the matrix $\mathbf{R}(x_j, y_j)$ for position (x_j, y_j) located at the center of each cell j, is built and stored in advance. This enables to reasonably approximate the matrix $\mathbf{R}\left(x_k^i, y_k^i\right)$ by the nearest cell position matrix $\mathbf{R}\left(x_j, y_j\right)$. Here, the number of particles is also chosen to be equal to the number of cells, i.e., $N_p = 6155$ and the degeneracy threshold N_{thres} is set to $N_p/100 \approx 61$.

C. Localization results

Now we present the localization results obtained both on simulated and real data for the scenario described above with the different localization approaches mentioned earlier. Fig. 4b and Fig. 4d show the estimated root mean squared error

$$RMSE = \sqrt{(x_k - \hat{x}_k)^2 + (y_k - \hat{y}_k)^2} \tag{20}$$

for the target position at each time step k on real and simulated data, respectively. Tracking yields better estimation results compared with non-tracking MSF in both LOS and NLOS zones. It can be noted that the particle filter exploiting one Rx antenna information converges quite slowly towards the right trajectory in the middle of the NLOS zone. On the contrary, in case of a particle filter using 4 Rx antennas, good localization results are obtained on the whole target trajectory and it reaches a lower variance compared to the single Rx antenna case.

To better analyze the above localization results, Fig. 5 shows the real data localization maps in the research domain at three time steps $k = 1, 5$ and 17, all corresponding to instants at which the target is actually in NLOS. As mentioned earlier, particle weights are updated proportionally to the likelihood of the measurement, i.e., the MSF cost function, according to (17). However, in case of using one single Rx antenna, the MSF output exhibits strong ambiguities, i.e., false positions which yield high likelihood values as depicted in Fig. 5a. Thus, particles corresponding to these false positions are granted high weight values. The particle cloud is then misled and converges quickly to the wrong zone after a few measurements, thus losing the true target position (Fig. 5e). The estimated location progressively comes back to the true target trajectory when ambiguities are reduced (Fig. 5f), that explains the slow convergence not helped by the resampling mechanism. On the contrary, in case of using 4 Rx, it can be observed that MSF ambiguities (Fig. 5g) are much lower compared with the one Rx case thanks to the contribution of the DoA information. Thus, the particle cloud converges early

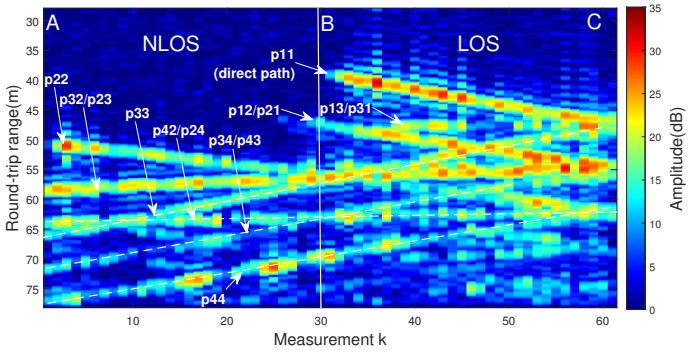

(a) Observation vectors (real data)

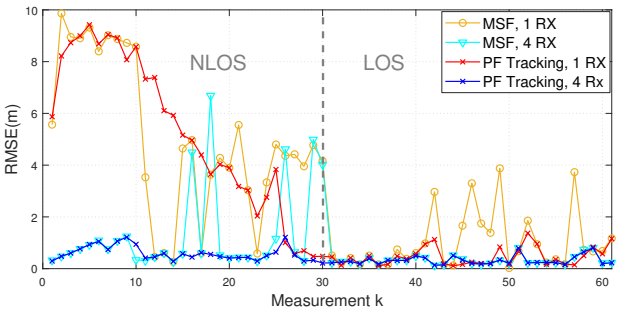

(b) Localization error (real data)

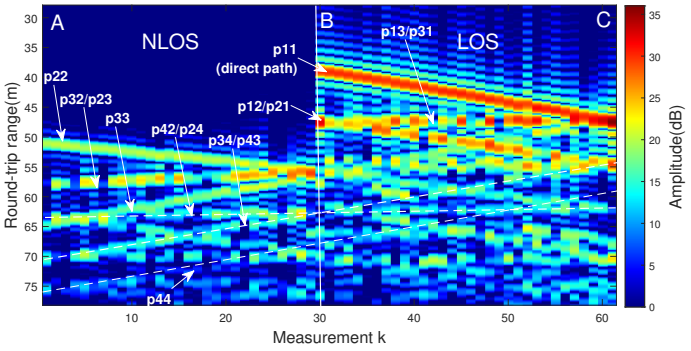

(c) Observation vectors (simulated data)

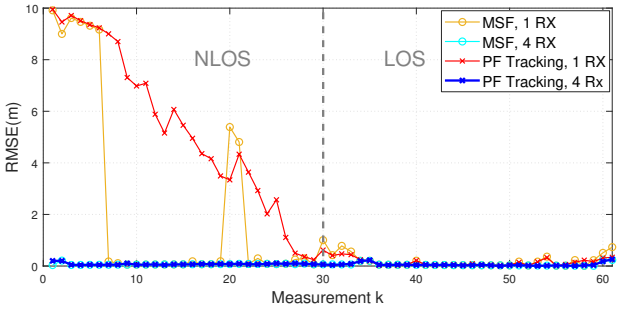

(d) Localization error (simulated data)

Fig. 4: Observation vector and corresponding localization error computed at each measurement/time step k for non-tracking MSF algorithm and proposed particle filter, for one Rx antenna.(a), (b): real data. (c) and (d): simulated data

towards the right trajectory and successfully tracks it over the whole recording (Fig. 5k and Fig. 5l).

V. Conclusion

In this paper, we propose an improved solution for estimating the position of a single NLOS target using an array of receiving antennas with the GLRT particle filter. Results from simulations and experiments demonstrate that incorporating DoA information allows for correcting estimation errors, particularly at the beginning of the target's trajectory. Our future work aims to enhance the tracking performance by optimizing the choice of importance density and exploring extensions of the approach to multi-target scenarios.

References

[1] A. Sume, M. Gustafsson, M. Herberthson, A. Janis, S. Nilsson, J. Rahm, A. Orbom, "Radar Detection of Moving Targets Behind Corners," in IEEE Transactions on Geoscience and Remote Sensing, vol. 49, no. 6, pp.2259-2267, 2011.

[2] T. Johansson, A. O¨ rbom, A. Sume, J. Rahm, S. Nilsson, M. Herberthson, M. Gustafsson, and A. Andersson, "Radar measurements of moving objects around corners in a realistic scene," in Proceedings of SPIE, Radar Sensor Technology, 2014, vol. 9077.

[3] O. Rabaste, E. Colin-Koeniguer, D. Poullin, A. Cheraly, J.F. Petex, H.K. Phan, "Around-the-corner radar: detection of a human being in non-line of sight", IET Radar, Sonar & Navigation, 2015, 9, (6), pp. 660–668.

[4] T. Johansson, Å. Andersson, M. Gustafsson and S. Nilsson, "Positioning of moving non-line-of-sight targets behind a corner," 2016 European Radar Conference (EuRAD), 2016, pp. 181-184.

[5] H. Du, C. Fan, Z. Chen, C. Cao, and X. Huang, "NLOS Target Localization with an L-Band UWB Radar via Grid Matching," Progress In Electromagnetics Research M, Vol. 97, 45-56, 2020.

[6] S. Fan, Y. Wang, G. Cui, S. Li, S. Guo, M. Wang, L. Kong, "Moving Target Localization Behind L-shaped Corner With a UWB Radar," 2019 IEEE Radar Conference (RadarConf), 2019, pp. 1-5.

[7] K. Thai, O. Rabaste, J. Bosse, D. Poullin, I. Hinostroza, T. Letertre, T. Chonavel, "Detection–Localization Algorithms in the Around-the-Corner Radar Problem," in IEEE Transactions on Aerospace and Electronic Systems, vol. 55, no. 6, pp. 2658-2673, 2019.

[8] L. L. Scharf and B. Friedlander, "Matched subspace detectors," in IEEE Transactions on Signal Processing, vol. 42, no. 8, pp. 2146-2157, 1994.

[9] A. J. Weiss, "Direct Geolocation of Wideband Emitters Based on Delay and Doppler," in IEEE Transactions on Signal Processing, vol. 59, no. 6, pp. 2513-2521, 2011.

[10] K. Thai, O. Rabaste, J. Bosse and T. Chonavel, "GLRT Particle Filter for Tracking Nlos Target in Around-the-Corner Radar," 2018 IEEE International Conference on Acoustics, Speech and Signal Processing (ICASSP), pp. 3216-3220, 2018.

[11] M. S. Arulampalam, S. Maskell, N. Gordon and T. Clapp, "A tutorial on particle filters for online nonlinear/non-Gaussian Bayesian tracking," in IEEE Transactions on Signal Processing, vol. 50, no. 2, pp. 174-188, Feb. 2002.

[12] O. Rabaste, C. Riché and A. Lepoutre, "Long-time coherent integration for low SNR target via particle filter in Track-Before-Detect," 2012 15th International Conference on Information Fusion, Singapore, 2012, pp. 127-134.

[13] B. Pham, O. Rabaste, J. Bosse, I. Hinostroza and T. Chonavel, "On the reduction of localization ambiguities of hidden target in the around-the-corner radar," CIE Conference on Radar, 2021 (in press).

[14] G. Storvik, "Particle filters for state-space models with the presence of unknown static parameters," in IEEE Transactions on Signal Processing, vol. 50, no. 2, pp. 281-289, 2002.

[15] A. Lepoutre, O. Rabaste and F. Le Gland, "Optimized instrumental density for particle filter in Track-Before-Detect," 9th IET Data Fusion Target Tracking Conference (DFTT 2012): Algorithms Applications, London, 2012.

[16] https://www.analog.com/en/design-center/evaluation-hardware-and-software/evaluation-boards-kits/eval-tinyrad.html

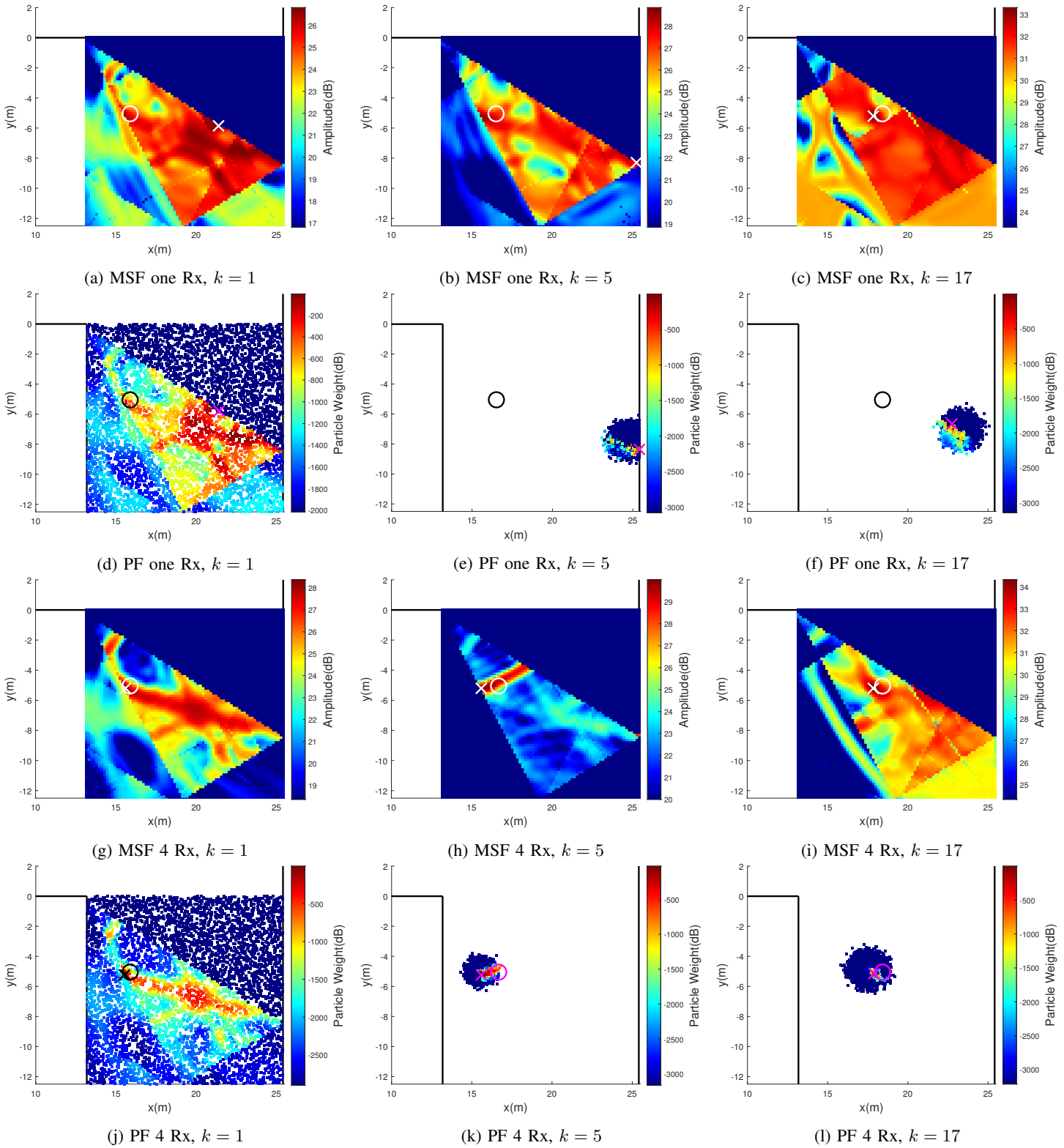

(a) MSF one Rx, $k = 1$ (b) MSF one Rx, $k = 5$ (c) MSF one Rx, $k = 17$

(d) PF one Rx, $k = 1$ (e) PF one Rx, $k = 5$ (f) PF one Rx, $k = 17$

(g) MSF 4 Rx, $k = 1$ (h) MSF 4 Rx, $k = 5$ (i) MSF 4 Rx, $k = 17$

(j) PF 4 Rx, $k = 1$ (k) PF 4 Rx, $k = 5$ (l) PF 4 Rx, $k = 17$

Fig. 5: Real data localization maps in the search domain at some measurements/time steps k of the particle filter (PF) and the Matched Subspace Filter (MSF) in case of using one Rx antenna and 4 Rx antennas. The true target position is marked by a circle; the estimated position is marked by a cross.